

# RETRACTED ARTICLE: LncRNA HLA Complex Group 11 Knockdown Alleviates Cisplatin Resistance in Gastric Cancer by Targeting the miR-144-3p/UBE2D1 Axis

Yu Li<sup>1,\*</sup>  
 Liqin Wang<sup>2,\*</sup>  
 Xiaoyi Xu<sup>3</sup>  
 Heng Sun<sup>1</sup>  
 Leilei Wu<sup>4</sup>

<sup>1</sup>Department of Oncology, First Affiliated Hospital, Heilongjiang University of Chinese Medicine, Harbin City, Heilongjiang Province, 150040, People's Republic of China; <sup>2</sup>Nursing Teaching and Research Department, First Affiliated Hospital, Heilongjiang University of Chinese Medicine, Harbin City, Heilongjiang Province, 150040, People's Republic of China; <sup>3</sup>Department of Medical Laboratory, First Clinical Medical College, Mudanjiang Medical University, Mudanjiang City, Heilongjiang Province, 157011, People's Republic of China; <sup>4</sup>Pharmacy Laboratory, College of Pharmacy, Mudanjiang Medical University, Mudanjiang City, Heilongjiang Province, 157011, People's Republic of China

\*These authors contributed equally to this work

**Objective:** Cisplatin (DDP) treatment is one of the most predominant chemotherapeutic strategies for patients with gastric cancer (GC). LncRNA noncoding RNA HLA complex group 11 (lncRNA HCG11) has been confirmed to promote GC progression. This study attempted to investigate the underlying molecular mechanism of HCG11 in DDP resistance of GC.

**Methods:** qRT-PCR was performed to evaluate the expression of HCG11, microRNA-144-3p (miR-144-3p), and ubiquitin-conjugating enzyme E2D1 (UBE2D1) in GC. The correlation between HCG11 and clinicopathological features of GC patients was assessed. DDP-resistant GC cells and their parental cells were cultured in different concentrations of DDP. The role of HCG11 for the viability and the half maximal inhibitory concentration (IC<sub>50</sub>) of DDP in DDP-resistant GC cells was determined by MTT assay. Then, the invasion of DDP-resistant GC cells was measured by transwell assay. Next, a dual-luciferase reporter assay was used to confirm the interaction among HCG11, miR-144-3p, and UBE2D1 in GC.

**Results:** The expression of HCG11 and UBE2D1 was elevated in tumor tissues of GC patients, but miR-144-3p was declined. HCG11 expression was elevated in DDP-resistant GC patients and is strongly correlated with DDP sensitivity and World Health Organization grade in GC patients. HCG11 knockdown reduced the viability, IC<sub>50</sub> of DDP, and invasion of DDP-resistant GC cells. Additionally, HCG11 targeted miR-144-3p and miR-144-3p further targeted UBE2D1. Feedback experiments indicated that low expression of miR-144-3p or overexpression of UBE2D1 mitigated the inhibitory effect of HCG11 depletion on DDP resistance of GC cells.

**Conclusion:** HCG11 knockdown attenuated DDP resistance of GC cells through via miR-144-3p/UBE2D1 axis, affording a novel therapeutic strategy for GC.

**Keywords:** gastric cancer, long noncoding RNA HCG11, microRNA-144-3p, UBE2D1, cisplatin resistance

## Introduction

Gastric cancer (GC) is a gastrointestinal tumor, and more than one million people are newly diagnosed with GC each year.<sup>1</sup> Although the mortality and incidence have decreased worldwide, the survival rate of GC patients remains unsatisfactory.<sup>2</sup> Cisplatin (DDP) generally serves as a first-line treatment for GC.<sup>3,4</sup> However, acquired drug resistance to DDP is a critical limitation to DDP-based treatment.<sup>5</sup> Thus, it is imperative to investigate the molecular mechanism involved in DDP resistance for GC therapy.

Correspondence: Leilei Wu  
 Pharmacy Laboratory, College of Pharmacy, Mudanjiang Medical University, Mudanjiang City, Heilongjiang Province, 157011, People's Republic of China  
 Tel +86 13766658535  
 Email Wuleilei725@163.com



Long noncoding RNAs (lncRNAs) modulate cellular processes in various gastrointestinal malignancies including GC.<sup>6,7</sup> In addition, lncRNAs elevation can lead to DDP resistance in GC. For instance, Dai et al have reported that lncRNA urothelial cancer-associated 1 (UCA1) elevation facilitates DDP resistance via recruiting enhancer of zeste homolog 2 (EZH2) in GC.<sup>8</sup> Xi et al have validated that up-regulation of lncRNA metastasis-associated lung adenocarcinoma transcript 1 (MALAT1) accelerates DDP resistance by enhancing autophagy-related protein 5 (ATG5) in GC.<sup>9</sup> LncRNA HCG11 has been found to act as a key mediator in tumor progression. For instance, HCG11 is related to poor prognosis and displays oncogenic activity in hepatocellular carcinoma (HCC).<sup>10</sup> HCG11 knockdown plays an anti-tumor role in osteosarcoma via repression of cell proliferation and migration.<sup>11</sup> Notably, HCG11 has been confirmed to promote malignant development of GC cells.<sup>12</sup> However, the role of HCG11 in modulating DDP resistance in GC remains not well elucidated.

MicroRNAs (miRNAs) have been proved to take part in diverse cellular processes, such as tumorigenesis and chemoresistance.<sup>13</sup> Interestingly, miRNAs can also attenuate DDP resistance in GC. For example, miR-148a-3p overcomes DDP resistance in GC by inhibiting cyto-protective autophagy.<sup>14</sup> MiR-524-5p constrains SRY-related high-mobility-group box 9 (SOX9) to enhance the DDP sensitivity of GC cells.<sup>15</sup> It has been documented that miR-144-3p often participates in GC progression. miR-144-3p expression is inhibited in GC and is related to tumor node-metastasis (TNM) staging.<sup>16</sup> MiR-144-3p elevation attenuates the GC cell malignant behaviors through repressing Pre-B cell leukemia homeobox 3 (PBX3).<sup>17</sup> MiR-144-3p suppresses zinc finger E-box binding homeobox 1 (ZEB1) to promote radiosensitivity of GC cells.<sup>18</sup> However, the regulatory relationship between HCG11 and miR-144-3p in mediating DDP resistance in GC is still unknown.

Ubiquitin-conjugating enzyme E2 D1 (UBE2D1), a member of UBE2D family, is involved in the pathogenesis of several types of human diseases.<sup>19–21</sup> Numerous studies have reported that UBE2D1 is associated with different cancers. UBE2D1 is up-regulated in lung adenocarcinoma and acts as an independent unfavorable prognostic biomarker.<sup>22</sup> Overexpression of UBE2D1 accelerates HCC progression and is related to poor prognosis in HCC patients.<sup>23</sup> Notably, UBE2D1 is closely associated with the overall survival coupled with low-risk in GC.<sup>24</sup> Despite these researches, the interactions among HCG11, miR-144-3p, and UBE2D1 to regulate DDP resistance in GC remains undefined.

Herein, HCG11 expression and its potential role in modulation of DDP resistance in GC were assessed. Besides, HCG11/miR-144-3p/UBE2D1 axis in GC pathogenesis was evaluated. This study may provide an approach to constrain DDP resistance in GC treatment.

## Materials and Methods

### Clinical Samples

Fifty-one GC patients who underwent gastrectomy between December 2016 and October 2018 at our hospital were recruited for the study. GC tissues (n = 51, cancer group) and paired adjacent non-tumor tissues (n = 51, normal group) were stored at  $-80^{\circ}\text{C}$ . Prior to gastrectomy, no radiotherapy or chemotherapy treatment was administered to the patients. Additionally, patients were also divided into DDP sensitivity (n = 24) and DDP resistance (n = 27) groups. DDP resistance was defined as tumor relapse during DDP-based chemotherapy after gastrectomy, and DDP sensitivity was defined as no tumor recurrence during DDP-based therapy. This study was performed in line with the principles of the Declaration of Helsinki. Approval was granted by the Ethics Committee of First Affiliated Hospital, Heilongjiang University of Chinese Medicine. Informed consent was obtained from all individual participants included in the study.

### Cell Culture

Human GC cell lines (AGS and MKN45) and human fetal gastric epithelial cell line (GES-1) were obtained from American Type Culture Collection (Manassas, VA, USA). AGS/DDP and MKN45/DDP cells were selected from AGS and MKN45 cells after stable exposure to the stepwise elevating levels of DDP for one year, and eventually maintained the final concentration of DDP (10  $\mu\text{M}$ ) in cell culture. Cells were cultured in DMEM (Invitrogen, Carlsbad, CA, USA) containing 10% FBS (Invitrogen) at  $37^{\circ}\text{C}$  with 5%  $\text{CO}_2$ .

### Cell Transfection

The short hairpin RNA (sh)-HCG11, sh-UBE2D1, sh-negative control (NC), miR-144-3p mimics, miR-NC, miR-144-3p inhibitor, inhibitor NC, pcDNA3.1 (pcDNA)-UBE2D1, and pcDNA-NC were obtained by Genepharma (Shanghai, China). AGS, AGS/DDP, MKN45, and MKN45/DDP cells grown to 85% confluence were transfected with these above agents using Lipofectamine 3000 reagent (Invitrogen).

## Quantitative Real-Time Polymerase Chain Reaction (qRT-PCR) and Western Blotting

qRT-PCR and Western blot were performed as previously described.<sup>25</sup> GAPDH, U6, and  $\beta$ -actin were used for the normalization of HCG11, miR-144-3p, and UBE2D1, respectively. The primer sequences are shown in Table 1. The antibodies (Sigma, St. Louis, MO, USA) for Western blot analysis were as follows: anti-UBE2D1 (1:1000, av43006), -Bax (1:1000, SAB3500343), -Bcl-2 (1:1000, PRS3335), and -GAPDH (1:5000, SAB2701826), and the HRP conjugate secondary antibody (1:5000, 12–348). The immunoblots were measured using an electrochemiluminescent detection system and quantified using ImageLab software.

## Detection of DDP Resistance in GC Cells

The resistance of GC cells to DDP was evaluated at half maximal inhibitory concentration (IC<sub>50</sub>). AGS, AGS/DDP, MKN45, and MKN45/DDP cells were cultured in the absence or presence of different levels of the DDP (0.1, 1, 5, 10, 20, 40, 80, and 160  $\mu$ M) for 72 h. Cell viability was measured by MTT assay kit (Sigma). Simply, cells were further cultured for 0, 24, 48, and 72 h, and then treated with 20  $\mu$ L of MTT (5 mg/mL). After incubation for 4 h, medium was removed and 100  $\mu$ L DMSO was added. The Optical density (OD) was measured. Cell survival rate was calculated as:  $(OD_{\text{treated group}} - OD_{\text{empty control group}}) / (OD_{\text{normal cell control group}} - OD_{\text{empty control group}}) \times 100\%$ . At last, the IC<sub>50</sub> of cells to DDP was calculated with reference to relative survival curves.

**Table 1** Primers sequences

Name of Primer	Sequences (5'-3')
HCG11-F	AGGAGTGGTTGCATTTGGGA
HCG11-R	CCCACCACGCAGTGAATAGT
GAPDH-F	TGACTTCAACAGCGACACCCA
GAPDH-R	CACCCGTGTGCTGTAGCCAAA
miR-144-3p-F	GCCCCTACAGTATAGATGATGTA
miR-144-3p-R	GTGCAGGGTCCGAGGT
U6-F	TGACACGCAAATTCGTGAAGCGTTC
U6-R	CCAGTCTCAGGGTCCGAGGTATTC
UBE2D1-F	GGACCTGTGGGAGATGACTTG
UBE2D1-R	TGGTACTAAGGGGTCATCTGGA
$\beta$ -actin-F	CATGTACGTTGCTATCCAGGC
$\beta$ -actin-R	CTCCTTAATGTCACGCACGAT

## Transwell Assay

For transwell assay, AGS/DDP and MKN45/DDP cells ( $2 \times 10^5$  cells) in serum-free medium were placed into upper chambers pre-coated with matrigel (Sigma). Medium with 10% FBS was added to the lower chambers. At 48 h post-incubation, cells in the upper chamber were wiped with cotton swab, while cells in the lower chambers were fixed with methanol, stained with 0.1% crystal violet, and then counted under an inverted light microscope (Olympus, Japan).

## Mouse Xenograft Tumor Model

Twenty BALB/c nude mice (6 weeks) were purchased from Esebio (Shanghai, China). All animal experiments were approved by the Animal Care and Use Committee of the First Affiliated Hospital, Heilongjiang University of Chinese Medicine. MKN45/DDP cells ( $5 \times 10^6$  cells) infected with lentivirus carrying sh-NC or sh-HCG11 was intravenously injected into mice. One week later, mice were further intraperitoneally injected with DDP (5 mg/kg) in PBS or PBS alone three times per week. Thus, mice were divided into the sh-HCG11 + PBS, sh-NC + PBS, sh-HCG11 + DDP, and sh-NC + DDP groups (n = 5). Tumor volume was detected one week after inoculation, and calculated using the following formula:  $1/2LW^2$  (L, length; W, width). After measurement of tumor volume, mice were anesthetized and sacrificed by cervical dislocation, and the tumor was collected and weighted.

## Bioinformatics Analysis

The gene expression analysis for TCGA cohort of GC was obtained from GEPIA2. The gene expression analysis for GSE22598, GSE79973, and GSE29272 cohorts of GC were downloaded from GEO. StarBase and LncBase were used to predict the targets of HCG11. A total of 4 miRNAs were determined by both two prediction tools. Only miR-144-3p expression in DDP-resistant GC cells declined considerably compared to their parental cells. Thus, miR-144-3p was selected as the candidate miRNA. Additionally, TargetScan software predicted UBE2D1 (total context++ score = -0.92) as one of the potential target genes of miR-144-3p. In parallel, UBE2D1 was also confirmed using miRDB (target score = 100). Thus, UBE2D1 was selected in this study.

## Dual-Luciferase Reporter Assay

The 3'-untranslated region (UTR) of HCG11 or UBE2D1 containing the potential binding sites of miR-144-3p was

inserted into 3' UTR of F-Luc in pGL3-Basic vectors (Ke Lei Biological Technology, Shanghai, China) to construct the HCG11 wild type (wt) or UBE2D1 wt. Similarly, the 3'-UTR segment of HCG11 or UBE2D1, including the mutated binding sequence of miR-144-3p, was cloned in pGL3-Basic vectors (Ke Lei Biological Technology) to generate the HCG11 mutant (mut) or UBE2D1 mut. AGS/DDP and MKN45/DDP cells were co-transfected with the above luciferase vectors and miR-NC or miR-144-3p mimics using Lipofectamine 3000 (Invitrogen).

## Statistical Analysis

GraphPad Prism 7.0 was used for statistical analyses. Data were presented as mean  $\pm$  standard deviation (SD). Variances among the groups were compared by Student's t-test or one-way ANOVA followed by Tukey's multiple comparisons test. The correlation significance was determined by Pearson correlation analysis. Differences were considered statistically significant at  $P < 0.05$ .

## Results

### HCG11 Was Clearly Elevated in DDP-Resistant GC

As shown in **Figure 1A** and **B**, HCG11 expression in GC tissues was visibly elevated compared with normal tissues in dataset GSE22598 ( $P < 0.001$ ) and GSE79973 ( $P = 0.024$ ). HCG11 was dramatically up-regulated in GC tissues ( $P < 0.001$ , **Figure 1C**). Additionally, HCG11 expression was considerably raised in TNM III/IV and DDP-resistant GC tissues ( $P < 0.001$ , **Figure 1D** and **E**). HCG11 expression was noticeably correlated with DDP sensitivity and World Health Organization (WHO) grade in GC patients ( $P < 0.01$ , **Table 2**). Kaplan–Meier survival curve indicated that high expression of HCG11 showed poor prognosis in GC patients (log rank  $P = 0.006$ , **Figure 1F**). Furthermore, HCG11 expression was considerably enhanced in AGS and MKN45 cells compared with GES-1 cells ( $P < 0.01$ ). In particular, DDP-resistant GC cells (AGS/DDP and MKN45/DDP) displayed higher HCG11 expression than their parental cells ( $P < 0.01$ , **Figure 1G**).

### HCG11 Silencing Alleviated the Resistance to DDP in GC Cells

As shown in **Figure 2A**, we found that the survival rate of AGS/DDP and MKN45/DDP cells was visibly elevated in contrast to their parental cells ( $P < 0.01$ ). Afterwards, sh-HCG11 or sh-NC was successfully transfected into AGS/

DDP and MKN45/DDP cells ( $P < 0.01$ , **Figure 2B**). In addition, MTT assay discovered that HCG11 knockdown significantly decreased AGS/DDP and MKN45/DDP cell viability ( $P < 0.01$ , **Figure 2C**). Moreover, sh-HCG11 could notably reduce IC50 of DDP in AGS/DDP and MKN45/DDP cells ( $P < 0.01$ , **Figure 2D**). The DDP at a concentration of IC50 (AGS/DDP cells, 71.34  $\mu$ M; MKN45/DDP cells, 61.28  $\mu$ M) was used for further experiments. Bax and Bcl-2 are biomarkers of apoptosis. As illustrated in **Figure 2E**, the protein expression of Bax was remarkably elevated, while Bcl-2 was declined in AGS/DDP and MKN45/DDP cells following sh-HCG11 transfection or DDP treatment ( $P < 0.01$ ). Compared with the sh-HCG11 group, the protein expression of Bax was markedly increased, while Bcl-2 was decreased in AGS/DDP and MKN45/DDP cells in the sh-HCG11 + DDP group ( $P < 0.01$ ). HCG11 silencing effectively enhanced the effects of DDP on the Bax and Bcl-2 protein expression in AGS/DDP and MKN45/DDP cells ( $P < 0.01$ ). As displayed in **Figure 2F**, transwell assay revealed that HCG11 inhibition or treatment with DDP could markedly decrease the invasion of AGS/DDP and MKN45/DDP cells ( $P < 0.01$ ). Compared with the sh-HCG11 group, AGS/DDP and MKN45/DDP cell invasion were significantly inhibited in the sh-HCG11 + DDP group ( $P < 0.01$ ). Sh-HCG11 could strengthen the hindering effect of DDP on cell invasion ( $P < 0.01$ ).

### HCG11 Suppression Attenuated the Resistance to DDP in a GC Mouse Model

The tumor xenograft of GC was established to further investigate the function of HCG11 in vivo. As displayed in **Figure 3**, both tumor volume and tumor weight were markedly reduced in the sh-HCG11 + PBS or sh-NC + DDP group, compared with the sh-NC + PBS group ( $P < 0.01$ ). In addition, the tumor volume and weight in the sh-HCG11 + DDP group were lower than that in the sh-HCG11 + PBS group ( $P < 0.01$ ). Moreover, HCG11 knockdown enhanced the inhibitory effect of DDP on the tumor growth ( $P < 0.01$ ).

### MiR-144-3p Was a Target of HCG11

A total of 4 miRNAs (miR-450b-5p, miR-532-3p, miR-144-3p, and miR-202-5p) were predicted as potential targets of HCG11 according to StarBase and LncBase (**Figure 4A**). In TCGA database, compared to the normal tissues, the expression of miR-450b-5p and miR-532-3p was increased, whereas miR-144-3p and miR-202-5p expression were evidently

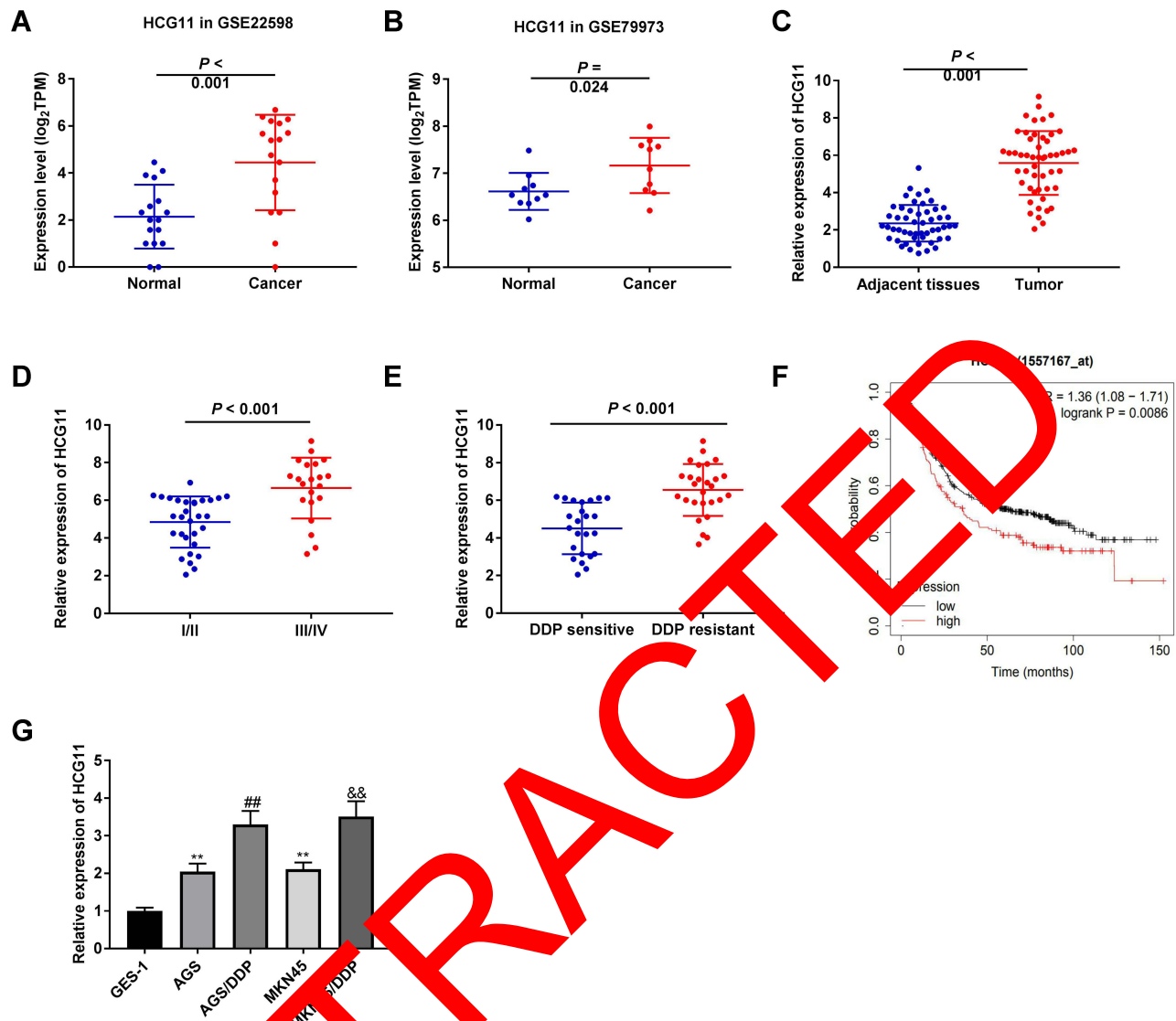


**Figure 1** HCG11 was clearly elevated in cisplatin (DDP)-resistant gastric cancer (GC) tissues and cells. **(A and B)** The gene expression analysis for the GSE22598 ( $P < 0.001$ ) and GSE79973 cohorts ( $P = 0.024$ ) of GC was obtained from Gene Expression Omnibus (GEO; <https://www.ncbi.nlm.nih.gov/geo/>); **(C)** The expression of HCG11 in adjacent tissues and tumor tissues of GC patients was measured by qRT-PCR.  $P < 0.001$  vs Adjacent tissues; **(D)** The expression of HCG11 in GC patients at the TNM I/II and TNM III/IV was detected by qRT-PCR.  $P < 0.001$  vs I/II; **(E)** Relative expression level of HCG11 in DDP-sensitive or DDP-resistant GC tissues was shown.  $P < 0.001$  vs DDP sensitive; **(F)** Kaplan-Meier survival curve for patients with high or low HCG11 expression. Logrank  $P = 0.0086$ ; **(G)** QRT-PCR was performed to reveal the expression of HCG11 in GES-1, AGS, AGS/DDP, MKN45, and MKN45/DDP cells. \*\* $P < 0.01$  vs GES-1, ## $P < 0.01$  vs AGS, && $P < 0.01$  vs MKN45.

repressed in GC tissues (Figure 4B). Notably, only miR-144-3p expression in AGS/DDP and MKN45/DDP cells was markedly suppressed by contrast to their parental cells ( $P < 0.05$ , Figure 4C). Therefore, miR-144-3p was selected as a candidate miRNA for further research. Figure 4D shows the binding site between HCG11 and miR-144-3p. HCG11 silencing could significantly increase miR-144-3p expression in AGS/DDP and MKN45/DDP cells ( $P < 0.01$ , Figure 4E). Overexpression of miR-144-3p significantly reduced the relative luciferase activity of the reporter with HCG11 WT in AGS/DDP and MKN45/DDP cells ( $P < 0.01$ , Figure 4F).

MiR-144-3p expression was considerably inhibited in GC tissues compared to adjacent tissues ( $P < 0.001$ , Figure 4G). Furthermore, a negative correlation between HCG11 and miR-144-3p expression was observed in GC patients ( $N = 51$ ,  $r = -0.4658$ ,  $P < 0.01$ , Figure 4H).

### MiR-144-3p Attenuated the Resistance to DDP in GC Cells

To explore the role of miR-144-3p in chemo-resistance to DDP in GC, miR-144-3p mimics/miR-NC or miR-144-3p

**Table 2** Correlation Between HCG11 Expression and Clinicopathological Features in Gastric Cancer Patients

Characteristics	n	HCG11		P value
		(Low) 25	(High) 26	
Age				0.482
<50 years	26	14	12	
≥50 years	25	11	14	
Gender				0.492
Male	22	12	10	
Females	29	13	16	
Diameter				0.069
<4 cm	24	15	9	
≥4 cm	27	10	17	
DDP Sensitivity				0.03**
Sensitive	24	17	7	
Resistant	27	8	19	
WHO Grade				0.02**
I + II	30	20	10	
III + IV	21	5		

Note: \*\*P < 0.01.

Abbreviation: WHO, World Health Organization.

inhibitor/inhibitor NC was initially transfected into AGS/DDP and MKN45/DDP cells, respectively (P < 0.01, Figure 5A). MiR-144-3p elevation markedly constrained the viability of AGS/DDP and MKN45/DDP cells (P < 0.01, Figure 5B). Additionally, IC50 of DDP in AGS/DDP and MKN45/DDP cells was clearly declined by miR-144-3p overexpression (P < 0.01, Figure 5C). miR-144-3p overexpression or DDP treatment considerably elevated Bax protein expression (P < 0.01) as well as inhibited Bcl-2 protein expression (P < 0.05) in AGS/DDP and MKN45/DDP cells. Compared with the miR-144-3p mimics group, the protein level of Bax was markedly increased, while Bcl-2 was decreased in AGS/DDP and MKN45/DDP cells in the miR-144-3p mimics + DDP group (P < 0.01). MiR-144-3p up-regulation could significantly potentiate the effects of DDP on Bax and Bcl-2 protein expression in AGS/DDP and MKN45/DDP cells (P < 0.01). As exhibited in Figure 5E, miR-144-3p elevation or treatment with DDP could markedly decline the invasion of AGS/DDP and MKN45/DDP cells (P < 0.01). Compared with the miR-144-3p mimics group, the invasion of AGS/DDP and MKN45/DDP cells was significantly suppressed in the miR-144-3p mimics + DDP group (P < 0.01). MiR-144-3p overexpression could lead to a marked decrease in invasion in the presence of DDP (P < 0.01, Figure 5E).

## MiR-144-3p Modulated the UBE2D1 Expression

The UBE2D1 was predicted as the potential miR-144-3p target by TargetScan and miRDB. TargetScan illustrated that miR-144-3p binds to the 3'UTR of UBE2D1 (Figure 6A). The relative luciferase activity of the reporter with UBE2D1 WT in AGS/DDP and MKN45/DDP cells was significantly repressed following miR-144-3p elevation (P < 0.01, Figure 6B). TCGA database and dataset GSE29272 displayed that UBE2D1 expression was evidently enhanced in GC tissues (P < 0.001, Figure 6C and D). Interestingly, UBE2D1 expression was remarkably elevated in GC tissues compared to that of adjacent tissues (P < 0.001, Figure 6E). An inverse correlation between the expression of miR-144-3p and UBE2D1 in GC patients was exhibited (N = 51, r = -0.4543, P < 0.01, Figure 6F). Moreover, miR-144-3p elevation could visibly suppress UBE2D1 protein expression in AGS/DDP and MKN45/DDP cells (P < 0.01, Figure 6G).

## HCG11 Inhibition Attenuated DDP Resistance via Modulating miR-144-3p/UBE2D1 Axis in GC Cells

As exhibited in Figure 7A, UBE2D1 expression was up-regulated in AGS and MKN45 cells (P < 0.01), was relatively high in AGS/DDP (P < 0.05) and MKN45/DDP

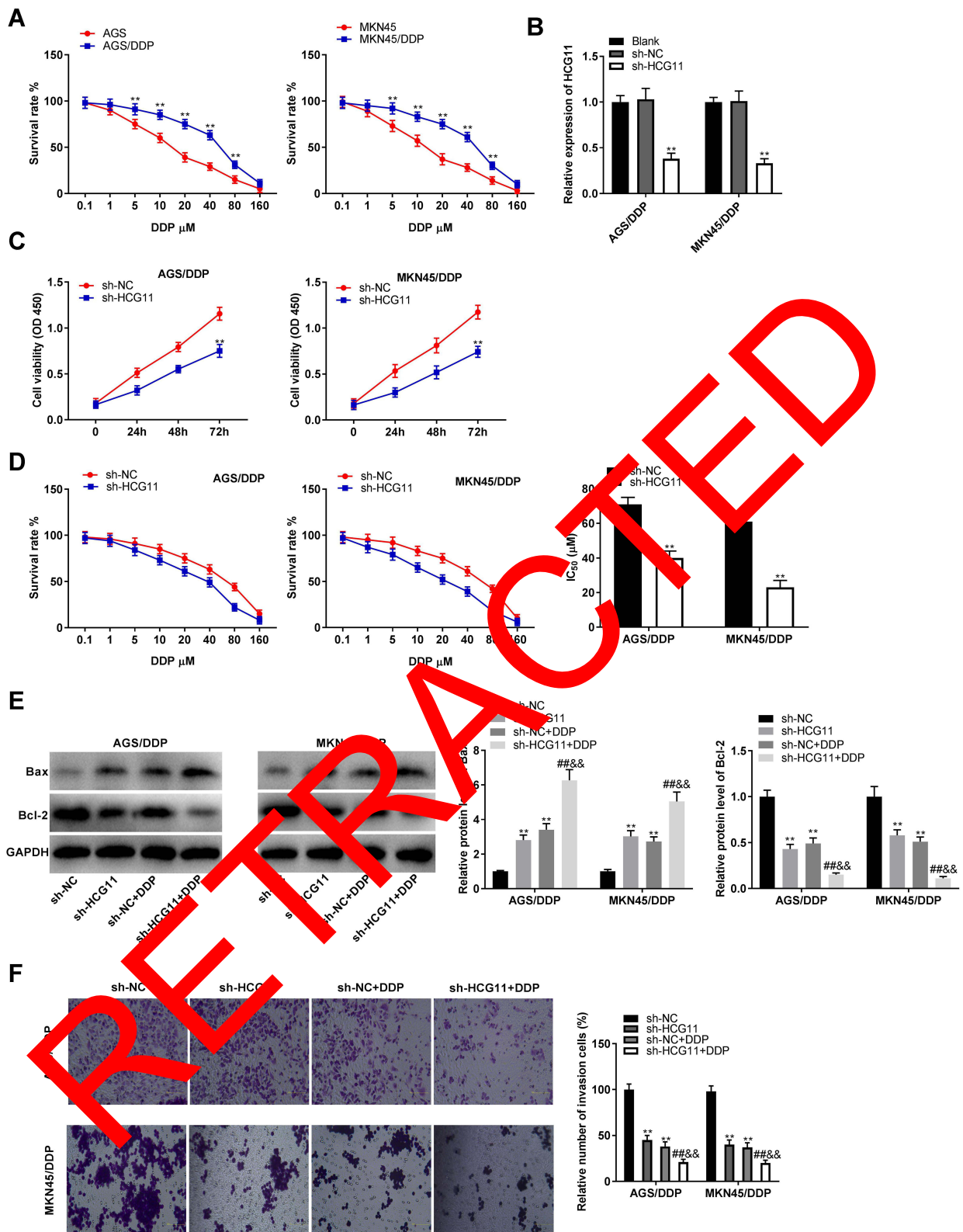


**Figure 2** HCG11 silencing alleviated the resistance to cisplatin (DDP) in gastric cancer (GC) cells. **(A)** The survival rate of DDP-resistant GC cells (AGS/DDP and MKN45/DDP) and their parental cells (AGS and MKN45) treated with a series dose (0.1, 1, 5, 10, 20, 40, 80, 160  $\mu$ M) of DDP was determined using MTT assay. \*\*P < 0.01 vs AGS or MKN45; **(B)** The transfection efficiency of sh-NC and sh-HCG11 were demonstrated by using qRT-PCR in AGS/DDP and MKN45/DDP cells. \*\*P < 0.01 vs sh-NC; **(C)** The viability of AGS/DDP and MKN45/DDP cells was measured by MTT assay. \*\*P < 0.01 vs sh-NC; **(D)** The effect of HCG11 knockdown on the IC<sub>50</sub> of DDP in AGS/DDP and MKN45/DDP cells was evaluated. \*\*P < 0.01 vs sh-NC; **(E)** The protein expression of Bax (pro-apoptotic protein) and Bcl-2 (anti-apoptotic protein) was used for evaluating apoptosis of AGS/DDP and MKN45/DDP cells according to Western blot. \*\*P < 0.01 vs sh-NC, ###P < 0.01 vs sh-HCG11, &P < 0.01 vs sh-NC + DDP; **(F)** Number of invasion cells was examined by transwell assay and the invasion rate was calculated. \*\*P < 0.01 vs sh-NC, ###P < 0.01 vs sh-HCG11, &P < 0.01 vs sh-NC + DDP.

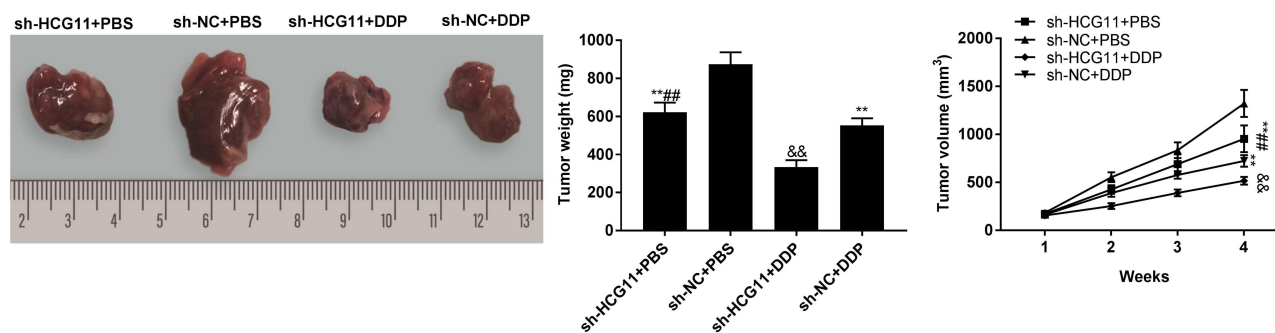


**Figure 3** HCG11 suppression attenuated the resistance to cisplatin (DDP) in gastric cancer (GC) tumors. Knockdown of HCG11 enhanced the inhibitory effects of DDP on GC tumor volume and tumor weight. \*\* $P < 0.01$  vs sh-NC + PBS, ### $P < 0.01$  vs sh-HCG11 + DDP, && $P < 0.01$  vs sh-NC + DDP.

DDP ( $P < 0.01$ ) cells relative to their parental cells. Then, UBE2D1 expression was effectively enhanced or inhibited after transfection of pcDNA-UBE2D1 or sh-UBE2D1 into MKN45/DDP cells ( $P < 0.01$ , Figure 7B). As shown in Figure 7C–E, we found that UBE2D1 inhibition not only markedly reduced the viability, IC<sub>50</sub> of DDP, Bcl-2 protein expression, and invasion rate but also increased Bax protein expression in MKN45/DDP cells ( $P < 0.01$ ). To further explore the molecular mechanism by which HCG11 inhibition attenuated the resistance of GC cells to DDP, rescue experiments were performed. Down-regulation of miR-144-3p or up-regulation of UBE2D1 could significantly reverse the inhibiting effects of sh-HCG11 on viability, IC<sub>50</sub> of DDP, Bcl-2 protein expression, and invasion rate, as well as weakened the promoting effect of sh-HCG11 on Bax protein expression in MKN45/DDP cells ( $P < 0.01$ ).

## Discussion

DDP resistance seriously limits the overall clinical efficacy of GC patients.<sup>26,27</sup> The enhanced lncRNAs expression has been regarded as a critical contributor of DDP resistance in various cancers, such as lncRNA X-inactive specific transcript (XIST) in lung adenocarcinoma,<sup>28</sup> lncRNA nuclear paraspeckle assembly transcript 1 (NEAT1) in ovarian cancer,<sup>29</sup> and lncRNA AK022798 in GC.<sup>30</sup> In the current study, HCG11 expression was significantly up-regulated in DDP-resistant GC tissues and cell lines. Furthermore, high HCG11 expression was significantly associated with DDP sensitivity and WHO grade in GC patients. Previously described noncoding RNAs were similar to HCG11. For instance, the lncRNA breast cancer anti-estrogen resistance 4 (BCAR4) expression is enhanced in GC tissues and has a correlation with clinical stage, leading to the DDP resistance.<sup>31</sup> Elevated expression of lncRNA plasmacytoma

variant translocation 1 (PVT1) is observed in DDP-resistant GC patients and is related to DDP sensitivity in GC.<sup>32</sup> Circular RNA AKT3 is positively associated with clinical stage, histological grade, and DDP resistance in GC patients.<sup>33</sup> Overall, we speculate that HCG11 overexpression may also be correlated with the DDP resistance in GC.

Increasing research has confirmed that aberrant expression of lncRNAs is tightly associated with therapeutic DDP resistance in GC. For example, lncRNA HOX transcript antisense RNA (HOTAIR) inhibits DDP sensitivity of GC cell lines, and accelerates multidrug-resistance genes expression.<sup>34</sup> lncRNA prostate cancer-associated transcript 1 (PCAT-1) silencing decreases the IC<sub>50</sub> of DDP, induces cell apoptosis in GC cells.<sup>35</sup> In this study, HCG11 depletion repressed viability and invasion, and facilitated apoptosis in DDP-resistant GC cells. Similarly, Zhang et al reported that HCG11 silencing restrains cell growth and contributes to the apoptosis of GC.<sup>12</sup> Additionally, our results indicated that HCG11 depletion not only decreased the IC<sub>50</sub> of DDP but also strengthened the reduction effect of DDP on malignant development of DDP-resistant GC cells. Taken together, we demonstrated that silencing of HCG11 may retard the progression of GC by overcoming DDP resistance. Moreover, HCG11 suppression clearly restrained the growth of tumor xenograft and sensitized mice to DDP treatment, indicating that HCG11 deficiency constrained the tumorigenesis of GC via attenuating DDP resistance in vivo.

Certain lncRNAs modulate miR-144-3p to participate in the progression of different human cancers. For instance, HCG11 silencing retards cell proliferation in ovarian cancer through enhancing miR-144-3p.<sup>36</sup> lncRNA SOX21 antisense RNA 1 (SOX21-AS1) accelerates cell invasion and suppresses cell apoptosis in glioma by inhibiting miR-144-3p.<sup>37</sup> Notably, lncRNA LINC00265 negatively regulates miR-144-3p to



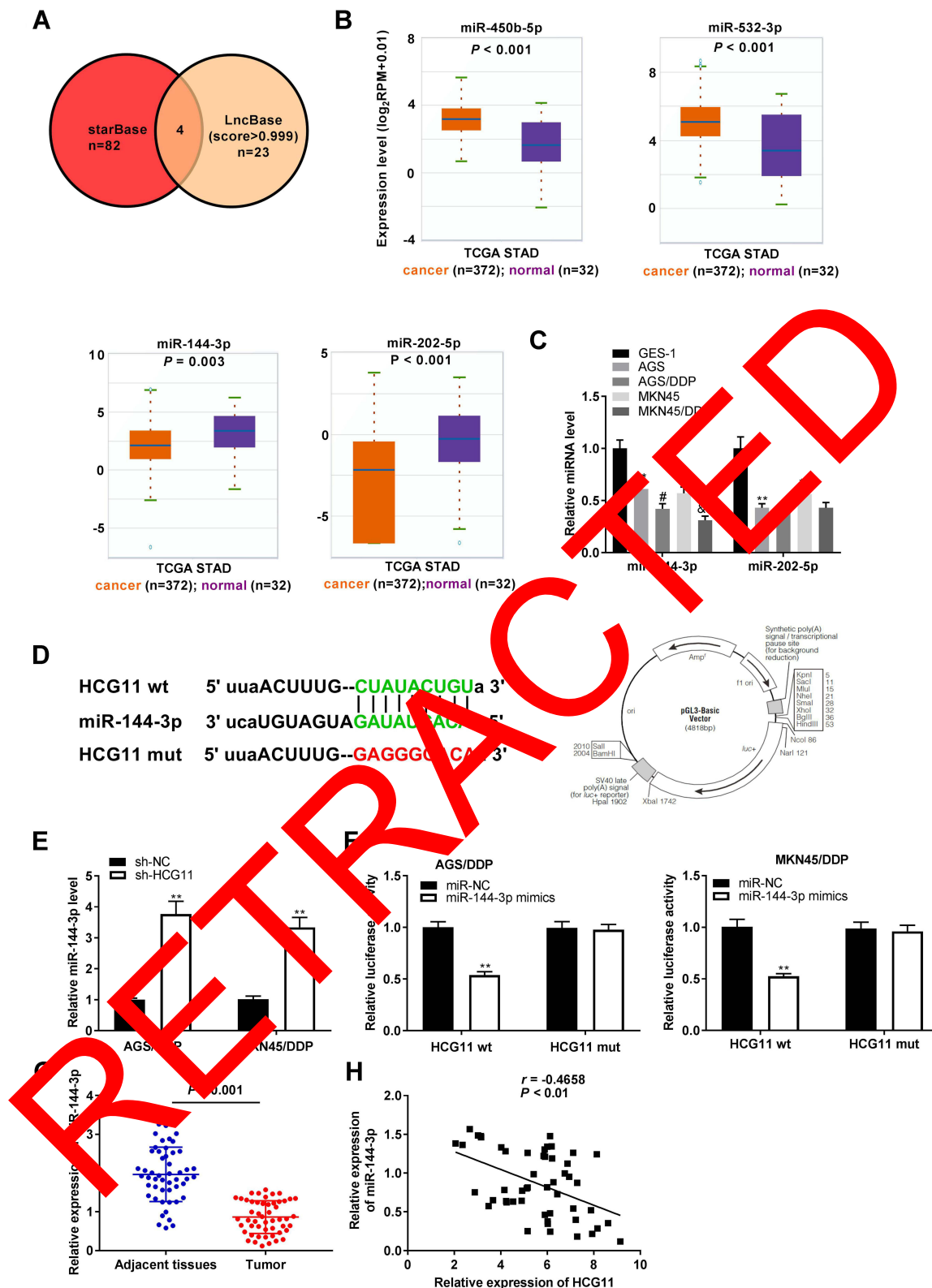


**Figure 4** MiR-144-3p served as a target of HCG11. (A) Total 82 miRNAs were predicted by StarBase and 23 miRNAs with a score > 0.999 were predicted by LncBase; (B) The gene expression analysis for the Cancer Genome Atlas (TCGA) cohort of gastric cancer (GC) was obtained from GEPIA2 (<http://gepia2.cancer-pku.cn>); (C) The expression of miR-144-3p and miR-202-5p was measured by qRT-PCR in GES-1, AGS, AGS/DDP, MKN45, and MKN45/DDP cells. \*\* $P < 0.01$  vs GES-1, # $P < 0.05$  vs AGS, && $P < 0.01$  vs MKN45; (D) Starbase exhibited the predicted binding site between HCG11 and miR-144-3p; The detailed physical structures of the luciferase assay plasmids; (E) QRT-PCR was conducted to detect the expression of miR-144-3p in AGS/DDP and MKN45/DDP cells. \*\* $P < 0.01$  vs sh-NC; (F) Relative luciferase activity in AGS/DDP and MKN45/DDP cells was measured by dual-luciferase reporter assay. \*\* $P < 0.01$  vs miR-NC; (G) The expression of miR-144-3p in adjacent tissues and tumor tissues in GC patients was examined by qRT-PCR.  $P < 0.001$  vs adjacent tissues; (H) The expression of HCG11 was negatively correlated with miR-144-3p in GC patients.  $P < 0.01$ ,  $r = -0.4658$ .

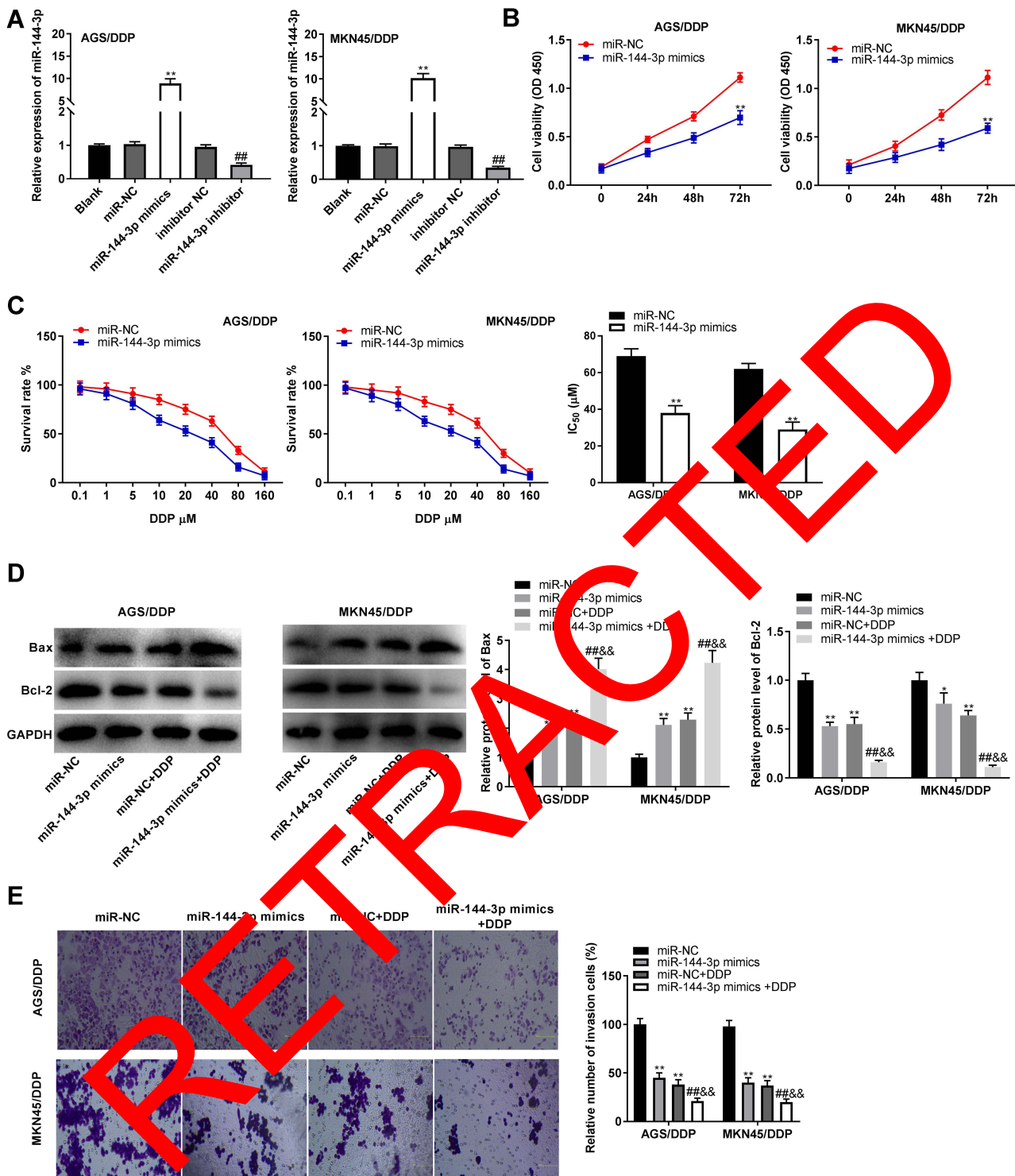


**Figure 5** MiR-144-3p attenuated the resistance to cisplatin (DDP) in gastric cancer (GC) cells. **(A)** QRT-PCR was used to evaluate the transfection efficiency of miR-NC, miR-144-3p mimics, inhibitor NC, and miR-144-3p inhibitor in AGS/DDP and MKN45/DDP cells. **(B)** The viability of AGS/DDP and MKN45/DDP cells transfected with miR-144-3p mimics or miR-NC was detected by MTT assay. **(C)** The effect of miR-144-3p overexpression on the IC<sub>50</sub> of DDP in AGS/DDP and MKN45/DDP cells was assessed. **(D)** The protein expression of Bax and Bcl-2 in AGS/DDP and MKN45/DDP cells was detected by Western blot. **(E)** The invasion rate in AGS/DDP and MKN45/DDP cells transfected with miR-144-3p mimics or miR-NC in the presence or absence of DDP was examined by transwell assay.

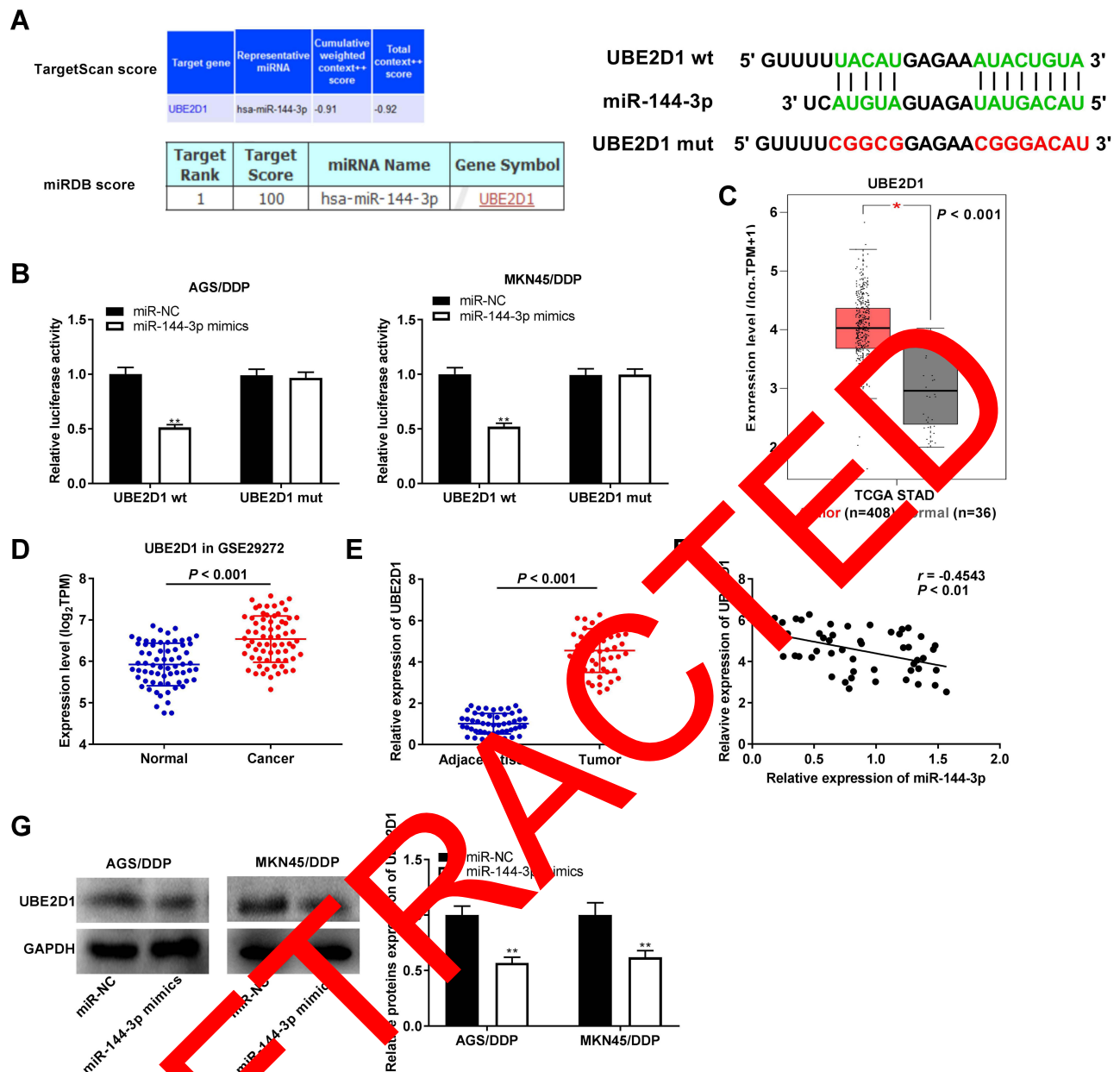


**Figure 6** MiR-144-3p modulates the UBE2D1 expression. (A) UBE2D1 was predicted as a potential miR-144-3p target by TargetScan and miRDB. TargetScan showed the predicted binding site between UBE2D1 and miR-144-3p; (B) Dual-luciferase reporter assay was performed to measure the relative luciferase activity in AGS/DDP and MKN45/DDP cells. \*\* $P < 0.01$  vs miR-NC; (C) The gene expression analysis for the Cancer Genome Atlas (TCGA) cohort of gastric cancer (GC) was obtained from GEPIA2 (<http://gepia2.cancer-pku.cn/>). \* $P < 0.001$  vs normal; (D) The gene expression analysis for the GSE29272 cohort of GC was obtained from Gene Expression Omnibus (GEO; <https://www.ncbi.nlm.nih.gov/geo/>).  $P < 0.001$ ; (E) QRT-PCR was used to detect the expression of UBE2D1 in adjacent tissues and tumor tissues in GC patients.  $P < 0.001$  vs adjacent tissues; (F) The expression of UBE2D1 was negatively correlated with miR-144-3p in GC patients.  $P < 0.01$ ,  $r = -0.4543$ ; (G) The protein expression of UBE2D1 in AGS/DDP and MKN45/DDP cells was measured by Western blot. \*\* $P < 0.01$  vs miR-NC.

accelerate GC cell proliferation.<sup>38</sup> Here, miR-144-3p was confirmed to be a target of and negatively regulated by HCG11, suggesting that HCG11 may influence GC by targeting miR-144-3p. MiR-144-3p possesses close relationship with DDP sensitivity and malignant progression in cancer. Yin et al believed that miR-144-3p reverses DDP resistance of lung cancer via targeting Nrf2.<sup>39</sup> Liu et al revealed that miR-

144-3p up-regulation overcomes DDP resistances in thyroid carcinoma.<sup>40</sup> Notably, existing studies have verified that miR-144-3p constraints malignant behaviors of BC cells.<sup>17,18</sup> In our study, miR-144-3p reduced the viability, IC<sub>50</sub> of DDP, and invasion, and promoted the apoptosis in DDP-resistant GC cells. MiR-144-3p overexpression enhanced the reduction effect of DDP on tumorigenesis of DDP-resistant GC cells.

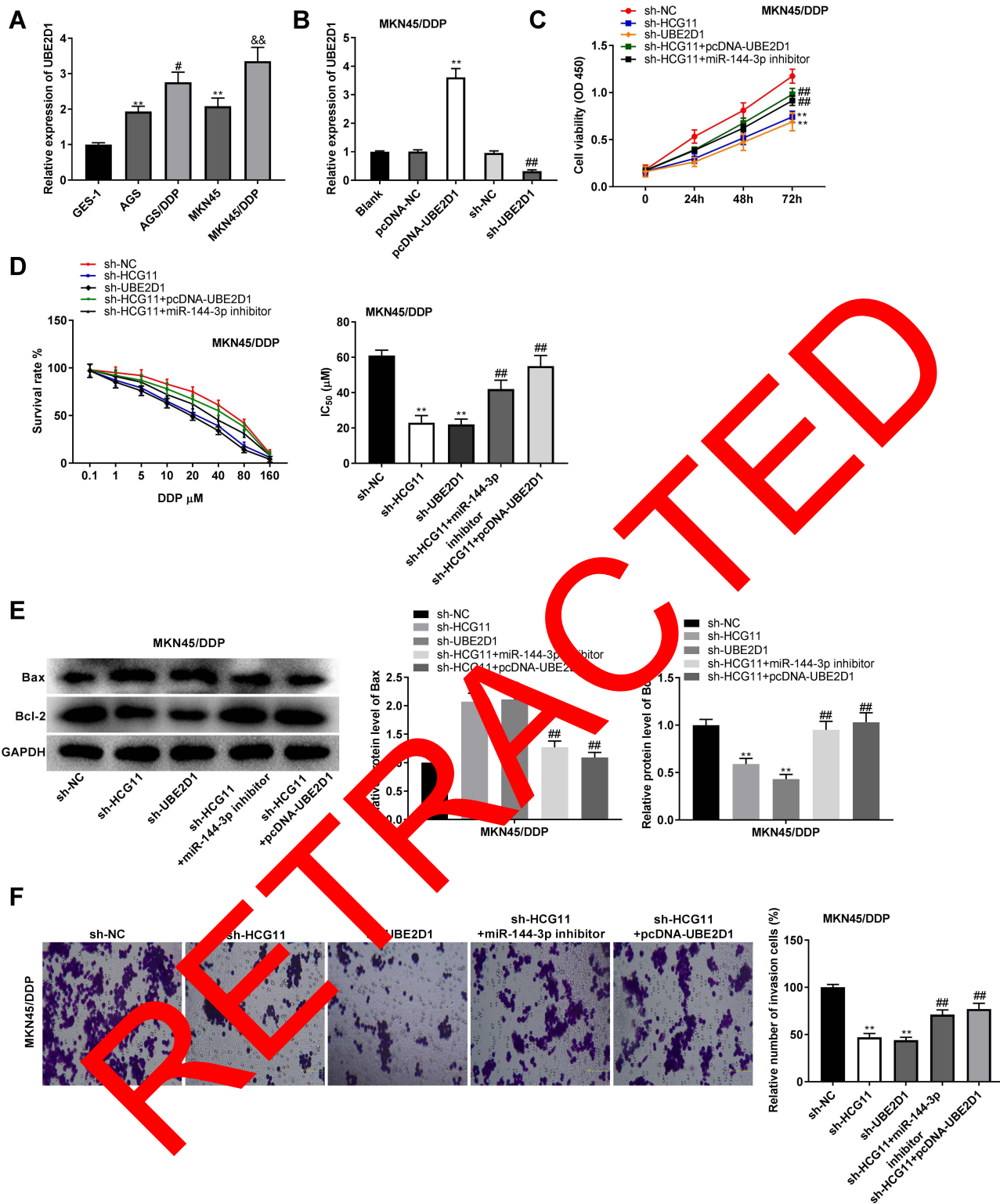


**Figure 7** HCG11 inhibition attenuated cisplatin (DDP) resistance via modulating miR-144-3p/UBE2D1 axis in gastric cancer (GC) cells. **(A)** QRT-PCR was performed to detect the expression of UBE2D1 in GES-1, AGS, AGS/DDP, MKN45, and MKN45/DDP cells. \*\*P < 0.01 vs GES-1, #P < 0.05 vs AGS, &&P < 0.01 vs MKN45; **(B)** The transfection efficiency of pcDNA-NC, pcDNA-UBE2D1, sh-NC, and sh-UBE2D1 in MKN45/DDP cells was measured by qRT-PCR. \*\*P < 0.01 vs pcDNA-NC, ###P < 0.001 vs sh-NC; **(C)** The cell viability of MKN45/DDP cells were determined by MTT assay. \*\*P < 0.01 vs sh-NC, ###P < 0.001 vs sh-HCG11; **(D)** The IC<sub>50</sub> of MKN45/DDP cells to DDP was calculated by relative survival curves. \*\*P < 0.01 vs sh-NC, ###P < 0.001 vs sh-HCG11; **(E)** The protein expression of Bax and Bcl-2 in MKN45/DDP cells was measured by Western blot. \*\*P < 0.01 vs sh-NC, ###P < 0.001 vs sh-HCG11; **(F)** The invasion rate of MKN45/DDP cells was examined by transwell assay. \*\*P < 0.01 vs sh-NC, ###P < 0.001 vs sh-HCG11.

Moreover, miR-144-3p inhibition clearly reversed the effect of HCG11 suppression exerted on GC cells. Thus, sh-HCG11 may attenuate the resistance to DDP in GC via up-regulating miR-144-3p.

UBE2D1 expression is usually highly expressed in tumors, such as lung adenocarcinoma,<sup>22</sup> HCC,<sup>23</sup> and osteosarcoma.<sup>41</sup> Similarly, UBE2D1 expression was notably elevated in GC in this study. Previous studies have verified that certain genes act as miR-144-3p targets to modulate GC progression. For examples, miR-144-3p represses Pre-B-cell leukemia homeobox 3 (PBX3) to hamper tumorigenesis of GC cells.<sup>17</sup> MiR-144-3p accelerates apoptosis and restrains proliferation of GC cells by suppressing ZEB1 expression.<sup>18</sup> Interestingly, Xing et al have reported that UBE2D1 is a potential target for gene therapy for GC.<sup>24</sup> In the present study, UBE2D1 was a target of inversely related to miR-144-3p, suggesting that miR-144-3p may be involved in GC tumorigenesis by blocking UBE2D1. Additionally, we further demonstrated that UBE2D1 knockdown reduced the viability, invasion and DDP resistance, and potentiated the apoptosis of MKN45/DDP cells, indicating that UBE2D1 is a key gene of DDP resistance in GC. Considering the interaction of HCG11 with miR-144-3p, we conjectured that HCG11 knockdown may suppress UBE2D1 in GC via up-regulating miR-144-3p. Encouragingly, rescue experiments indicated that UBE2D1 elevation attenuated the improved DDP sensitivity of DDP-resistant GC cells caused by HCG11 depletion. To sum up, HCG11 knockdown attenuated DDP-resistant GC cells to DDP by regulating the miR-144-3p/UBE2D1 axis in GC. In addition, many other HCG11-related axes are also confirmed to affect cancer progressions, such as HCG11-miR-144-3p-PBX3 axis in ovarian cancer,<sup>36</sup> HCG11-miR-26a-5p-PC12 axis in hepatocellular carcinoma,<sup>11</sup> and HCG11-miR-579-MMP13 axis in osteosarcoma.<sup>11</sup> Notably, the HCG11-miR-1276-CTNNB1-Wnt axis is also involved in the regulation of GC cell malignant biological behavior.<sup>12</sup> WNT pathway is one of the most important signaling pathways in cancers, and its activation is closely associated with DDP resistance in GC. For instances, Caveolin-1 increases the DDP resistance of GC cells by activating the WNT pathway.<sup>42</sup> Sinomenine sensitizes human GC cells to DDP through negative regulation of Wnt pathway.<sup>43</sup> LncRNA HOTAIR knockdown decreases DDP resistance of GC cells by inhibiting the WNT pathway.<sup>44</sup> Therefore, we speculated that HCG11 may influence WNT pathway to participate in the regulation

of the DDP resistance of GC cells. This aspect of research will be considered in our future studies.

There were also some other limitations in this study. First, this study only focused on HCG11, and the global expression profiles of lncRNAs between DDP-resistant and DDP-sensitive GC cases are needed. Second, the study on the role of HCG11-miR-144-3p-UBE2D1 axis was limited to the cellular level, and further in vivo experiments are needed.

## Conclusion

Collectively, HCG11 expression was elevated in DDP-resistant GC cells and tissue. Knockdown of HCG11 reduced the resistance to DDP in GC through sponge of miR-144-3p to mediate UBE2D1 expression. Our research may give a new therapeutic target to hinder DDP resistance in GC.

## Data Sharing Statement

The datasets used and/or analysed during the current study are available from the corresponding author on reasonable request.

## Ethics Approval and Informed Consent

This study was performed in line with the principles of the Declaration of Helsinki. Approval was granted by the Ethics Committee of First Affiliated Hospital, Heilongjiang University of Chinese Medicine. Informed consent was obtained from all individual participants included in the study. All experimental protocols were approved by the Ethics Committee of the First Affiliated Hospital, Heilongjiang University of Chinese Medicine. All procedures were performed in accordance with ethical standards and laboratory care and use guidelines of our hospital.

## Funding

There is no funding to report.

## Disclosure

Yu Li, Liqin Wang, Xiaoyi Xu, Heng Sun, and Leilei Wu declared that they have no conflicts of interest for this work.

## References

1. Thrift AP, El-Serag HB. Burden of gastric cancer. *Clin Gastroenterol Hepatol.* 2020;18(3):534–542.

2. Bray F, Ferlay J, Soerjomataram I, Siegel RL, Torre LA, Jemal A. Global cancer statistics 2018: GLOBOCAN estimates of incidence and mortality worldwide for 36 cancers in 185 countries. *CA Cancer J Clin*. 2018;68(6):394–424.
3. Yamada Y, Boku N, Mizusawa J, et al. Docetaxel plus cisplatin and S-1 versus cisplatin and S-1 in patients with advanced gastric cancer (JCOG1013): an open-label, Phase 3, randomised controlled trial. *Lancet Gastroenterol Hepatol*. 2019;4(7):501–510.
4. Lordick F, Kang YK, Chung HC, et al. Capecitabine and cisplatin with or without cetuximab for patients with previously untreated advanced gastric cancer (EXPAND): a randomised, open-label phase 3 trial. *Lancet Oncol*. 2013;14(6):490–499.
5. Verstraelen J, Reichl S. Multidrug resistance-associated protein (MRP1, 2, 4 and 5) expression in human corneal cell culture models and animal corneal tissue. *Mol Pharm*. 2014;11(7):2160–2171.
6. Yue B, Qiu S, Zhao S, et al. LncRNA-ATB mediated E-cadherin repression promotes the progression of colon cancer and predicts poor prognosis. *J Gastroenterol Hepatol*. 2016;31(3):595–603.
7. Xu W, He L, Li Y, Tan Y, Zhang F, Xu H. Silencing of lncRNA ZFAS1 inhibits malignancies by blocking Wnt/beta-catenin signaling in gastric cancer cells. *Biosci Biotechnol Biochem*. 2018;82(3):456–465.
8. Dai Q, Zhang T, Pan J, Li C. LncRNA UCA1 promotes cisplatin resistance in gastric cancer via recruiting EZH2 and activating PI3K/AKT pathway. *J Cancer*. 2020;11(13):3882–3892.
9. Xi Z, Si J, Nan J. LncRNA MALAT1 potentiates autophagy-associated cisplatin resistance by regulating the microRNA-30b/autophagy-related gene 5 axis in gastric cancer. *Int J Oncol*. 2019;54(1):239–248.
10. Li ML, Zhang Y, Ma LT. LncRNA HCG11 accelerates the progression of hepatocellular carcinoma via miR-26a-5p/ATG12 axis. *Eur Rev Med Pharmacol Sci*. 2019;23(24):10708–10720.
11. Wang L, Zhou J, Zhang Y, Hu T, Sun Y. Long non-coding RNA HCG11 aggravates osteosarcoma carcinogenesis via regulating the microRNA-579/MMP13 axis. *Int J Gen Med*. 2020;12(1):685–695.
12. Zhang H, Huang H, Xu X, et al. LncRNA HCG11 promotes proliferation and migration in gastric cancer via competing miR-1276/CTNBN1 and activating Wnt signaling pathway. *Gene Cell Int*. 2019;19(350):019–1046.
13. Di LG, Garofalo M, Croce CM. MicroRNAs in cancer. *Annu Rev Pathol*. 2014;9(2):287–314.
14. Li B, Wang W, Li Z, et al. MicroRNA-148a-3p enhances cisplatin cytotoxicity in gastric cancer through mitochondrial fission induction and cyto-protective autophagy suppression. *Cancer Lett*. 2017;410:212–227.
15. Wang J, Xue X, Hong H, et al. Upregulation of microRNA-524-5p enhances the cisplatin sensitivity of gastric cancer cells by modulating proliferation and metastasis by targeting SOX9. *Oncotarget*. 2017;8(1):574–582.
16. Sahami-Far M, H. Ghazali, L. Ghazali, Z. Nezhadi A. Expression levels of miR-144-3p and miR-144-3p in gastric cancer and their relationships with clinicopathological parameters. *Clin Lab*. 2020;66(6):200417.
17. Li B, Zhang S, Shen H, Li C. MicroRNA-144-3p suppresses gastric cancer progression by inhibiting epithelial-to-mesenchymal transition through targeting PBX3. *Biochem Biophys Res Commun*. 2017;484(2):241–247.
18. Gao ZY, Liu H, Zhang Z. miR-144-3p increases radiosensitivity of gastric cancer cells by targeting inhibition of ZEB1. *Clin Transl Oncol*. 2020;1(10):020–02436.
19. Mao D, Wu M, Wei J, Zhou X, Yang L, Chen F. MicroRNA-101a-3p could be involved in the pathogenesis of temporomandibular joint osteoarthritis by mediating UBE2D1 and FZD4. *J Oral Pathol Med*. 2020;13(10):13131.
20. Azzam SK, Osman WM, Lee S, et al. Genetic associations with diabetic retinopathy and coronary artery disease in Emirati patients with Type-2 diabetes mellitus. *Front Endocrinol*. 2019;10:283.
21. Liu H, Zhou J, Bi J, Yang W. Potential regulatory factors in the pathogenesis of ankylosing spondylitis. *Cell Mol Biol*. 2020;66(5):105–110.
22. Hou L, Li Y, Wang Y, et al. UBE2D1 RNA expression was an independent unfavorable prognostic indicator in lung adenocarcinoma, but not in lung squamous cell carcinoma. *Dis Markers*. 2018;21:4108919.
23. Zhou C, Bi F, Yuan J, Yang F, Sun S. Gain of UBE2D1 facilitates hepatocellular carcinoma progression and is associated with DNA damage caused by continuous IL-6. *J Exp Clin Cancer Res*. 2018;37(1):018–0951.
24. Xing C, Cai Z, Gong J, Zhou J, Xu J, et al. Identification of potential biomarkers involved in gastric cancer through integrated analysis of non-coding RNA associated competing endogenous RNAs network. *Clin Lab*. 2018;64(10):1661–1669.
25. Yuan H, Chen Z, Bai S, et al. Molecular mechanism of lncRNA SMARCC2/miR-551b-3p/TP53/PRSS4 axis in gastric cancer. *Cancer Lett*. 2018;418:84–96.
26. Lu Y, Han D, Liu W, et al. miR-158 confers cisplatin resistance in gastric cancer cells via activating Chk1 signaling pathway. *Cancer Biol Ther*. 2014;15(12):1128–1134.
27. Du Y, Zhu Y, Zhou Y, et al. miR-200c enhances cisplatin resistance of human gastric cancer cell line by targeting NFKBIB. *Tumour Biol*. 2016;37(12):1261–1269.
28. Song J, Pan LM, Chen LB, Wang Y. LncRNA XIST promotes human gastric adenocarcinoma cells to cisplatin resistance via let-7i/BAG-1 axis. *Cell Cycle*. 2017;16(21):2100–2107.
29. An L, Lv W, Zhang Y. LncRNA NEAT1 contributes to paclitaxel resistance of ovarian cancer cells by regulating ZEB1 expression via miR-194. *Oncol Targets Ther*. 2017;10:5377–5390.
30. Wang Q, Sun R, Jiang C, Li Y. Notch 1 promotes cisplatin-resistant gastric cancer formation by upregulating lncRNA AK022798 expression. *Anticancer Drugs*. 2015;26(6):632–640.
31. Wang L, Chunyan Q, Zhou Y, et al. BCAR4 increase cisplatin resistance and predicted poor survival in gastric cancer patients. *Eur Rev Med Pharmacol Sci*. 2017;21(18):4064–4070.
32. Zhang XW, Bu P, Liu L, Zhang XZ, Li J. Overexpression of long non-coding RNA PVT1 in gastric cancer cells promotes the development of multidrug resistance. *Biochem Biophys Res Commun*. 2015;462(3):227–232.
33. Huang X, Li Z, Zhang Q, et al. Circular RNA AKT3 upregulates PIK3R1 to enhance cisplatin resistance in gastric cancer via miR-198 suppression. *Mol Cancer*. 2019;18(1):71.
34. Yan J, Dang Y, Liu S, Zhang Y, Zhang G. LncRNA HOTAIR promotes cisplatin resistance in gastric cancer by targeting miR-126 to activate the PI3K/AKT/MRP1 genes. *Tumour Biol*. 2016;37(12):16345–16355.
35. Guo Y, Yue P, Wang Y, Chen G, Li Y. PCAT-1 contributes to cisplatin resistance in gastric cancer through miR-128/ZEB1 axis. *Biomed Pharmacother*. 2019;118:109255.
36. Li XF, Hu DM, Zhao YX, Zhang L, Jin Y. Knockdown of lncRNA HCG11 suppresses cell progression in ovarian cancer by modulating miR-144-3p/PBX3. *Eur Rev Med Pharmacol Sci*. 2020;24(21):11032–11040.
37. Gai SY, Yuan ZH. Long non-coding RNA SOX21-AS1 promotes cell proliferation and invasion through upregulating PAK7 expression by sponging miR-144-3p in glioma cells. *Neoplasma*. 2020;67(2):333–343.
38. Yang Z, OuYang X, Zheng L, Dai L, Luo W. Long intergenic noncoding RNA00265 promotes proliferation of gastric cancer via the microRNA-144-3p/Chromobox 4 axis. *Bioengineered*. 2021;19(10):1876320.

39. Yin Y, Liu H, Xu J, et al. miR-144-3p regulates the resistance of lung cancer to cisplatin by targeting Nrf2. *Oncol Rep.* 2018;40(6):3479–3488.
40. Liu F, Zhang J, Qin L, et al. Circular RNA EIF6 (Hsa\_circ\_0060060) sponges miR-144-3p to promote the cisplatin-resistance of human thyroid carcinoma cells by autophagy regulation. *Aging.* 2018;10(12):3806–3820.
41. Huang WT, Liu AG, Cai KT, et al. Exploration and validation of downregulated microRNA-199a-3p, downstream messenger RNA targets and transcriptional regulation in osteosarcoma. *Am J Transl Res.* 2019;11(12):7538–7554.
42. Wang X, Lu B, Dai C, et al. Caveolin-1 promotes chemoresistance of gastric cancer cells to cisplatin by activating WNT/ $\beta$ -catenin pathway. *Front Oncol.* 2020;10:46.
43. Liu Y, Liu C, Tan T, Li S, Tang S, Chen X. Sinomenine sensitizes human gastric cancer cells to cisplatin through negative regulation of PI3K/AKT/Wnt signaling pathway. *Anticancer Drugs.* 2019;30(10):983–990.
44. Cheng C, Qin Y, Zhi Q, Wang J, Qin C. Knockdown of long non-coding RNA HOTAIR inhibits cisplatin resistance of gastric cancer cells through inhibiting the PI3K/Akt and Wnt/ $\beta$ -catenin signaling pathways by up-regulating miR-34a. *Int J Biol Macromol.* 2018;107(Pt B):2620–2629.

RETRACTED

Cancer Management and Research

Dovepress

Publish your work in this journal

Cancer Management and Research is an international, peer-reviewed open access journal focusing on cancer research and the optimal use of preventative and integrated treatment interventions to achieve improved outcomes, enhanced survival and quality of life for the cancer patient.

The manuscript management system is completely online and includes a very quick and fair peer-review system, which is all easy to use. Visit <http://www.dovepress.com/testimonials.php> to read real quotes from published authors.

Submit your manuscript here: <https://www.dovepress.com/cancer-management-and-research-journal>